JOURNAL OF CATALYSIS 157, 145–152 (1995)

Quantum Mechanical Study of Ti/$MgCl_2$-Supported Ziegler–Natta Catalysts

J. S. Lin and C. R. A. Catlow

Davy Faraday Research Laboratory, The Royal Institution of Great Britain, 21 Albemarle Street, London W1X 4BS, UK

Received December 15, 1994; revised May 11, 1995; accepted May 26, 1995

Quantum mechanical methods using a point-charge embedded cluster technique have been applied to the Ti/$MgCl_2$-supported Ziegler-Natta catalyst to investigate how different oxidation states of Ti (III and IV) and different surface structures of the β-$MgCl_2$ crystal ((100) and (110) planes) influence the geometries and energetics of (i) Ti complexes adsorbed on the surfaces of the β-$MgCl_2$ crystal and (ii) the precoordinated-ethylene Ti complexes adsorbed on the same surfaces. Our calculations indicate that the Ti(III) complexes will be adsorbed on the surface of the (100) plane more strongly than those of Ti(IV). We also find that Ti(III) complexes bind more strongly to the (110) than to the (100) plane. Finally, our comparison of the energies of precoordinated-ethylene Ti complexes adsorbed on the different surfaces suggests that the atomic arrangement of the surfaces of the β-$MgCl_2$ crystal is crucial in stabilising such surface complexes. © 1995 Academic Press, Inc.

INTRODUCTION

Since the discovery of the heterogeneous Ti/$MgCl_2$-supported catalysts for Ziegler–Natta olefin polymerisation there have been extensive efforts to rationalise and understand the structure and behaviour of this catalytic system (1–3). The following two problems are of particular interest in the discussion of the polymerisation mechanism: first, the detail of the structure at the atomic level of the polymerisation centres present in the catalyst, and second, the nature of the interaction between these centres and olefin molecules. Indeed, these factors play a crucial role in determining the activity and stereospecificity of the olefin polymerisation reaction. The solution of these fundamental problems has, however, proceeded more slowly than the commercial development of these catalysts and even simple questions such as the surface structures of active $MgCl_2$ support and the oxidation states of Ti when adsorbed on these surface structures are still under discussion (4–10).

Our recent computer-modelling study (11) has established the nature of the surface structures of the β-$MgCl_2$ crystal and of the possible active sites created when Ti species are adsorbed on these surfaces to promote the precoordination of the olefin molecule to the Ti centre. However, this work, based on interatomic potential models, gives us only an approximate description of the structures and energies of the active sites. Also, the simulation approach employing interatomic potentials cannot provide further understanding of the reaction mechanisms involved during the polymerisation processes, such as the precoordination of olefin molecules to Ti unsaturated sites and the insertion of olefin molecules into the Ti–C bond. These processes involve the formation and breaking of bonds, in which case we must take into account explicit electronic structure effects.

Another recent study of Colbourn *et al.* (12) using the density functional theory approach has successfully modelled the $TiCl_4$ species adsorbed on the (100) surface of β-$MgCl_2$. However, this work, which used a 15-atom cluster to simulate the surface, did not consider the long-range electrostatic effect of the real surfaces which presumably will have a significant influence on the geometries and energies of the adsorbed $TiCl_4$ species.

In this study we therefore employ quantum mechanical methods with point-charge embedded clusters (13) to determine the structures of adsorbed Ti species on the surfaces of β-$MgCl_2$. Using these techniques we can further investigate how the different surface structures of the β-$MgCl_2$ crystal and different oxidation states of Ti centres influence first the nature of the interaction between the Ti centres and ethylene molecules and second the geometries and energies of the precoordinated ethylene Ti complexes adsorbed on the surfaces of the β-$MgCl_2$ crystal.

METHOD

The quantum mechanical method that we use in the present study to investigate embedded clusters is very similar to the standard electronic structure method based on the Hartree–Fock procedure for cluster calculations, except that the cluster is embedded within a finite point-charge array to account for the effects of the surrounding

0021-9517/95 $12.00

lattice. In the present study, both restricted Hartree–Fock, closed-shell (RHFCS) and open-shell (RHFOS) calculations were carried out using the GAMESS-UK program (14). Particular care must be paid to the embedding point charges in cluster calculations. It is necessary that the point-charge arrays are such that the electrostatic potential and fields within the cluster can be reproduced accurately and that the termination effects associated with the outermost atoms within the cluster and the boundaries of the point charges are minimal.

In order to reduce the computational requirement for the quantum mechanical calculations we applied the effective core potential (ECP) which allows us to exclude the core electrons and thereby simplify our calculations by dealing only with corresponding valence electrons. The ECP of Hay and Wadt (15) with the corresponding minimal (MIN) and double-zeta (DZ) valence basis sets (15) for Mg, Cl, Ti, and C, and STO-3G and double-zeta (DZ) basis sets for H have been used throughout this study. Test calculations were performed using all electron techniques with richer basis sets for the $TiCl_4$ molecule. The changes in bond lengths compared with those calculated using the pseudopotential and basis sets employed in this study were at most 0.02 Å, while the changes in adsorption energies on the (100) surface of β-$MgCl_2$ were less than 0.2 eV. Although highly accurate results may require richer basis sets and the inclusion of electron correlation, the techniques used here are sufficient to provide a good description of the problems of interest in this study.

RESULTS

Simulated Surfaces of β-$MgCl_2$ Crystal: (100) and (110) Planes

A cluster of Mg_2Cl_4 (illustrated in Fig. 1 was placed at the centre of the simulated surface of the (100) plane using a cluster of 189 point charges while one of Mg_3Cl_6 (illustrated in Fig. 2) was placed at the centre of the simulated surface of the (110) plane using a cluster of 417 point charges. Although the use of larger clusters might be desirable, the extra computational effort required would have greatly restricted the scope of this study. Also we found that the electronic changes in the surface ions involved by the adsorption of the Ti species are confined to a small number of atoms; clusters of the size used in this study are therefore acceptable provided they are properly embedded in a matrix of point charges which accurately reproduce the long-range electrostatic potential in the region of the adsorption site. The point-charge matrices were carefully chosen so as to achieve the necessary reproduction of electrostatic potential in the region of the adsorption site. As a result, the number of point charges required is different for the different surfaces and it is, moreover, necessary to relax the outermost point charges from the perfect lattice positions. We do not consider the surface of the (001) plane in this study because our previous simulation results (11) suggest that this surface is not a satisfactory support for stable adsorbed Ti complexes. For both clusters, the embedding point charge array ensures that both the electrostatic potentials and fields within the clusters are close to those of the real infinite surface.

The Hartree–Fock self-consistent field method was used to optimise partially the cluster geometry using a gradient technique. In this treatment the atoms which are the nearest neighbours of the point charges are fixed during the optimisation, owing to the difficulties arising from the lack of the pair electron repulsion at the boundary between the point charges and the SCF treated cluster. With this approximation our optimised structural parameters for clusters of Mg_2Cl_4 and Mg_3Cl_6 are in reasonable agreement with our computer-modelling results (11), as shown in Tables 1a and 1b. The approximation is not expected to have

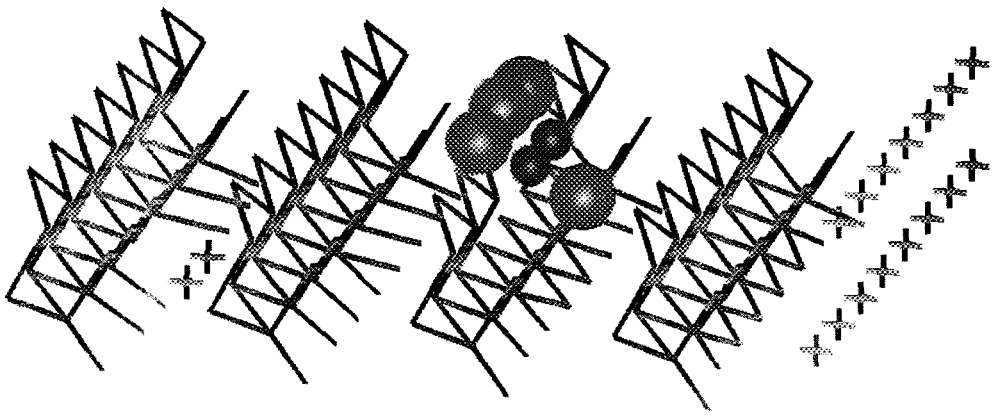

FIG. 1. The model used to represent the (100) surface. A quantum mechanically described cluster of composition Mg_2Cl_4 is embedded in 189 point charges which reproduce the Madelung potential within the cluster due to the crystal. The large spheres are the Cl, the smaller spheres are Mg, and the remainder are point charges.

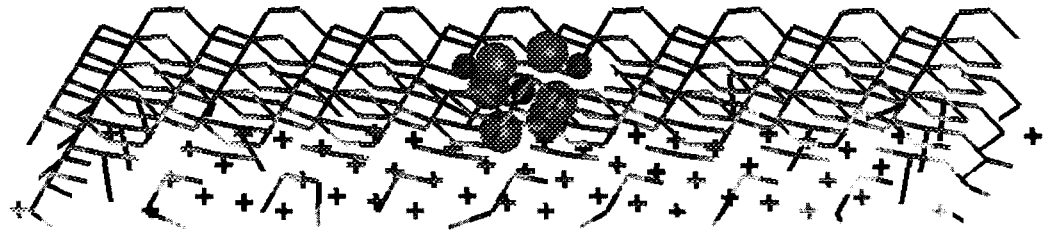

FIG. 2. The model used to represent the (110) surface. A quantum mechanically described cluster of composition Mg_2Cl_4, is embedded in 417 point charges.

any significant effect on the geometries and energies of Ti species adsorbed on these model surfaces.

Ti Species Adsorbed on the (100) Surface of the β-$MgCl_2$ Crystal

It is known that a reducing agent such as AlR_3 (R = CH_3) is needed to modify the oxidation state of Ti within the Ti/$MgCl_2$-supported Ziegler–Natta catalyst precursors for the olefin polymerisation reaction. However, from our previous simulation results we can confidently rule out Ti(II) complexes adsorbed on the surfaces of the β-$MgCl_2$ crystal as the possible active sites. We therefore investigated the possible precursors of the Ti species adsorbed on the (100) surface of the β-$MgCl_2$ crystal by carrying out calculations of the geometries and energies of adsorbed $TiCl_3R$ and $TiCl_2R$ (R = H, CH_3, and Cl) species on this surface. Calculations of the changes in energies accompanying these substitutions are also helpful in elucidating the effects of both steric and electrical factors on the adsorption energy.

The calculated structures of the *tetravalent* $TiCl_3R$ species adsorbed on the (100) surface are shown in Fig. 3. We expect that on substitution of one Cl in the $TiCl_4$ molecule by H and CH_3 ligands the effective charge on the Ti will change slightly, due to the different inductive effect of the H and CH_3 ligands compared to the Cl ligand. This minor change in the charge of the Ti has, however, little effect on the bonding of the $TiCl_3H$ species adsorbed on the (100) surface; indeed, the nature of the bonding between the $TiCl_3H$ species and the surface is dominated by the electrostatic interaction between the two Cl atoms in $TiCl_3H$ and the Mg atoms on the surface, as is the case for $TiCl_4$ species adsorbed on the same surface.

In contrast, the bond strength of the $TiCl_3CH_3$ species adsorbed on the (100) surface is much less, owing to the steric repulsion between the CH_3 ligand and the surface, as indicated by the short bond length (~2.70 Å) between the H in the CH_3 ligand and the Cl atoms on the surface. This is reflected in our calculated adsorption energy for the adsorbed $TiCl_3CH_3$ molecule on the (100) surface of β-$MgCl_2$, which is significantly less than the counterparts for adsorbed $TiCl_4$ and $TiCl_3H$ molecules on the same surface, as shown in Table 2.

Next we consider the structure of adsorbed *trivalent* $TiCl_2R$ molecules on the (100) surface of the β-$MgCl_2$ crystal, as shown in Fig. 4. We found first that there is no significant decrease in the adsorption energy when one Cl in the $TiCl_3$ molecule has been substituted by a CH_3 ligand. To explain this result we note that the $TiCl_2CH_3$ molecule will adsorb on the (100) surface in such a way as to have a CH_3 ligand pointing away from the surface. Therefore the steric repulsion between the CH_3 group and the surface will be unimportant. Moreover, we found that the $TiCl_2R$ molecules are adsorbed more strongly than $TiCl_3R$ on the (100) surface. To understand this interesting effect we first noted that the change in the structure from a slightly distorted tetrahedral $TiCl_3R$ to a slightly distorted trigonal

TABLE 1a

Calculated Structural Parameters for the Mg_2Cl_4 Cluster used in Simulating the (100) Surface of β-$MgCl_2$

Basis sets	Method	R_{Mg-Cl} (Å)	Mg–Cl–Mg (°)
MIN	RHFCS	2.466	91.351
DZ	RHFCS	2.428	92.897
	Simulation[a]	2.398	98.910

[a] From our previous study, Ref. (11), which was based on the use of energy minimisation techniques employing interatomic potentials.

TABLE 1b

Calculated Structural Parameters for the Mg_3Cl_6 Cluster used in Simulating the (110) Surface of β-$MgCl_2$

Basis sets	Method	R_{Mg-Cl} (Å)	Cl–Mg–Cl (°)
MIN	RHFCS	2.312	85.313
DZ	RHFCS	2.332	84.022
	Simulation[a]	2.348	85.199

[a] From our previous study, Ref. (11).

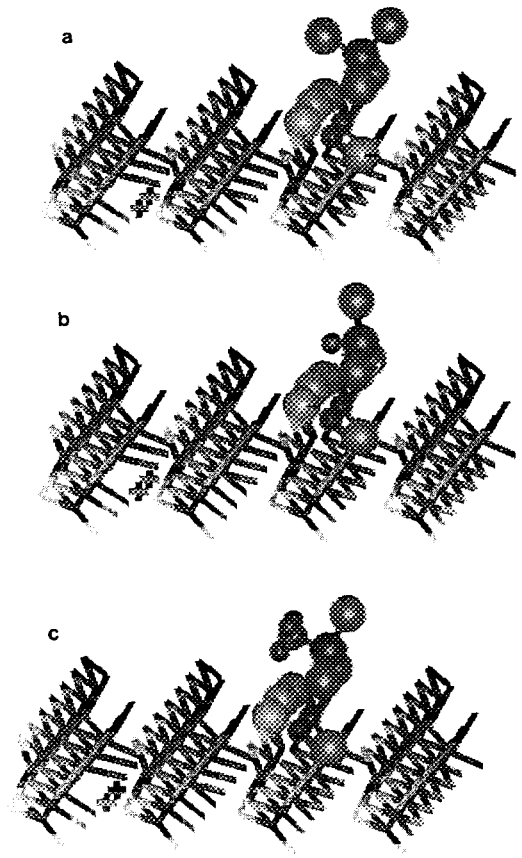

FIG. 3. The calculated structures of (a) $TiCl_4$, (b) $TiCl_3H$, and (c) $TiCl_3CH_3$ adsorbed on the (100) surface of the β-$MgCl_2$ crystal. The large dark spheres are Ti, the large light spheres are Cl; in the lowest diagram a CH_3 group is bonded to the Ti; the smallest spheres represent hydrogen.

TABLE 2

Calculated Structural Parameters and Adsorption Energies of Adsorbed $TiCl_3R$ (R = Cl, H, and CH_3) Molecules on the (100) Surface of β-$MgCl_2$

Species	Method/basis sets	$R_{Mg\ Cl}$ (Å)[a]	$R_{Cl\ Cl}$ (Å)[b]	E_{abs} (eV)[c]
$TiCl_4$	RHFCS/MIN	3.151	3.502	0.480
	RHFCS/DZ	3.055	3.527	0.453
$TiCl_3H$	RHFCS/MIN	3.048	3.484	0.571
	RHFCS/DZ	2.909	3.426	0.566
$TiCl_3CH_3$	RHFCS/MIN	2.970	3.451	0.180
	RHFCS/DZ	3.010	3.455	0.140

[a] The distance between the Mg atom on the surface and the Cl atom in the $TiCl_3R$.

[b] The distance between the Cl atom on the surface and the Cl atom in the $TiCl_3R$.

[c] E_{ads} is calculated by subtracting the total energy of the Ti species adsorbed on the surface from the total energies of both the Ti species and the simulated cluster surface.

planar $TiCl_2R$ complex increases the Cl_i–Ti–Cl_i bond angle (where Cl_i indicates the Cl atom of the complex interacting with the surface). This change will enhance the interaction between the chlorine atoms in the complex and the Mg atoms on the surface as they now match more closely the Mg–Mg separation on the surface. Indeed, our calculated smaller bond lengths for Mg–Cl_i, as shown in Table 3, are in line with this argument. Another reason for the greater stabilisation of the adsorbed $TiCl_2R$ complexes on the (100) surface is that the slight distortion of the trigonal planar $TiCl_2R$ complex will cause the Ti centre to interact with the Cl atom on the (100) surface. As a result there is electron transfer from the Cl atom on the surface to the Ti atom (which becomes even more receptive to the ethylene molecule, as will be discussed later). Finally, for the reasons discussed above, we do not expect any signifi-

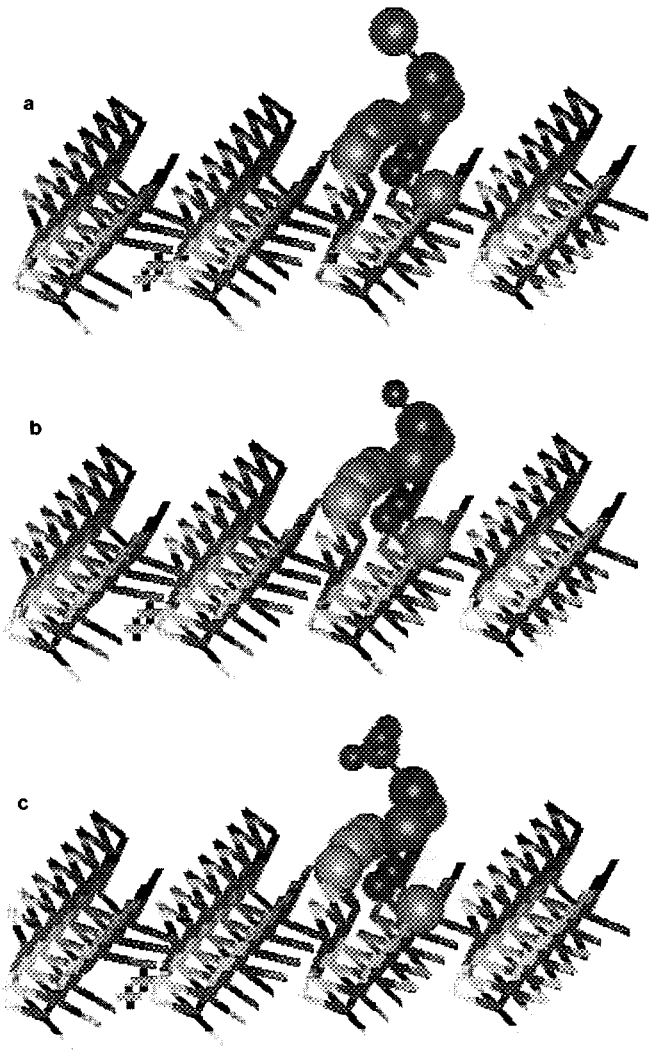

FIG. 4. The calculated structures of (a) $TiCl_3$, (b) $TiCl_2H$, and (c) $TiCl_2CH_3$ adsorbed on the (100) surface of the β-$MgCl_2$ crystal.

TABLE 3

Calculated Structural Parameters and Adsorption Energies of Adsorbed $TiCl_2R$ (R = Cl, H, and CH_3) Molecules on the (100) Surface of β-$MgCl_2$

Species	Method/basis sets	R_{Mg-Cl} (Å)[a]	R_{Cl-Cl} (Å)[b]	E_{abs} (eV)[c]
$TiCl_3$	RHFOS/MIN	2.708	3.469	1.159
	RHFOS/DZ	2.669	3.396	1.011
$TiCl_2H$	RHFOS/MIN	2.713	3.436	1.081
	RHFOS/DZ	2.642	3.287	1.015
$TiCl_2CH_3$	RHFOS/MIN	2.660	3.383	0.935
	RHFOS/DZ	2.611	3.269	0.895

[a] The distance between the Mg atom on the surface and the Cl atom in the $TiCl_2R$.

[b] The distance between the Cl atom on the surface and the Cl atom in the $TiCl_2R$.

[c] E_{ads} is again calculated by subtracting the total energy of the Ti species adsorbed on the surface from the total energies of both the Ti species and the simulated cluster surface.

cant change in the adsorption energies when substituting with H and CH_3 ligands as a result of modification of the oxidation state of Ti, as is indeed evident from the results reported in Table 3.

$TiCl_2R$ Species Adsorbed on the (110) Surface of the β-$MgCl_2$ Crystal

From the above results we have learned that the change of geometry from $TiCl_3R$ to $TiCl_2R$ accompanying the change of the oxidation state of Ti from IV to III will enhance the interaction between the Cl atoms in the $TiCl_2R$ complexes and the Mg atoms on the (100) surface of the β-$MgCl_2$ crystal. However, we must also investigate how the different surfaces of the β-$MgCl_2$ crystal interact with the Ti complexes. Therefore we carried out calculations to determine the geometries and energies of the $TiCl_2R$ species adsorbed on the (110) surface and to analyse the factors governing this interaction. The calculated structures are shown in Fig. 5; bond lengths and adsorption energies are reported in Table 4. It is easy to see that the optimisation of the interaction between the Cl_i atoms in the $TiCl_2R$ and the Mg atoms on the (110) surface will force the Cl_i–Ti–Cl_i bond angle in the $TlCl_2R$ molecule to increase significantly and allow a greater interaction between the Ti in the $TiCl_2R$ molecule and the surface Cl atoms. Indeed, our calculated Mulliken charges of the Cl atom on the (110) surface decrease to a greater extent than those of the Cl atom on the (100) surface, which suggests that there is even more electron transfer from the Cl atom on the (110) surface to the Ti centre, resulting in the Ti species having a higher adsorption energy on the (110) than on the (100) surface.

C_2H_4 Monomer Interacting with Ti Species Adsorbed on the (100) and (110) Surface

To initiate the polymerisation of C_2H_4 on the active sites of the Ti species adsorbed on the activated surfaces of $MgCl_2$-supported catalysts it is necessary to bring the C_2H_4 monomer into contact with the Ti species. Therefore we need to explore the manner in which the C_2H_4 monomer approaches the adsorbed Ti complexes. As discussed ear-

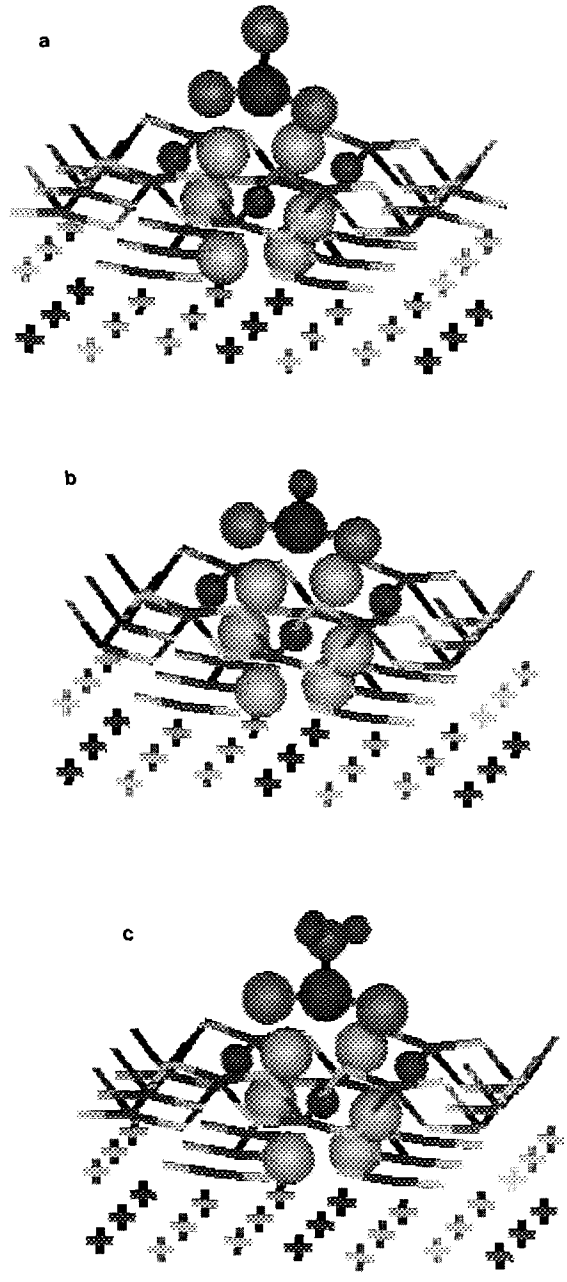

FIG. 5. The calculated structures of (a) $TiCl_3$, (b) $TiCl_2H$, and (c) $TiCl_2CH_3$ adsorbed on the (110) surface of the β-$MgCl_2$ crystal.

TABLE 4

Calculated Structural Parameters and Adsorption Energies of Adsorbed $TiCl_2R$ (R = Cl, H, and CH_3) Molecules on the (110) Surface of β-$MgCl_2$

Species	Method/basis sets	R_{Mg-Cl} (Å)[a]	R_{Cl-Cl} (Å)[b]	E_{abs} (eV)[c]
$TiCl_3$	RHFOS/MIN	2.579	2.845	1.394
	RHFOS/DZ	2.638	2.766	1.098
$TiCl_2H$	RHFOS/MIN	2.488	2.794	1.861
	RHFOS/DZ	2.579	2.678	1.411
$TiCl_2CH_3$	RHFOS/MIN	2.554	2.795	1.888
	RHFOS/DZ	2.546	2.715	1.608

[a] The distance between the Mg atom on the surface and the Cl atom in the $TiCl_2R$.

[b] The distance between the Cl atom on the surface and the Cl atom in the $TiCl_2R$.

[c] E_{ads} is calculated by subtracting the total energy of the Ti species adsorbed on the surface from the total energies of both the Ti species and the simulated cluster surface.

TABLE 5

Calculated Structural Parameters and Binding Energies of C_2H_4 Monomer Interacting with Adsorbed $TiCl_2R$ (R = H and CH_3) Molecules on the (100) Surface of β-$MgCl_2$

Species	Method/basis sets	R_{Ti-C} (Å)[a]	$R_{C=C}$ (Å)[b]	E_{bind} (eV)[c]
$C_2H_4/TiCl_2H$	RHFOS/MIN	2.670	1.461	1.456
	RHFOS/DZ	2.865	1.371	1.708
$C_2H_4/TiCl_2CH_3$	RHFOS/MIN	2.620	1.462	1.458
	RHFOS/DZ	2.707	1.371	1.505

[a] The distance between the middle point of the C=C double bond and the Ti atom in the $TiCl_2R$.

[b] The bond length of the C=C double bond.

[c] E_{bind} is calculated by subtracting the total energy of the Ti-C_2H_4 species adsorbed on the surface from the total energies of both the Ti species adsorbed on the surface and the isolated C_2H_4 molecule.

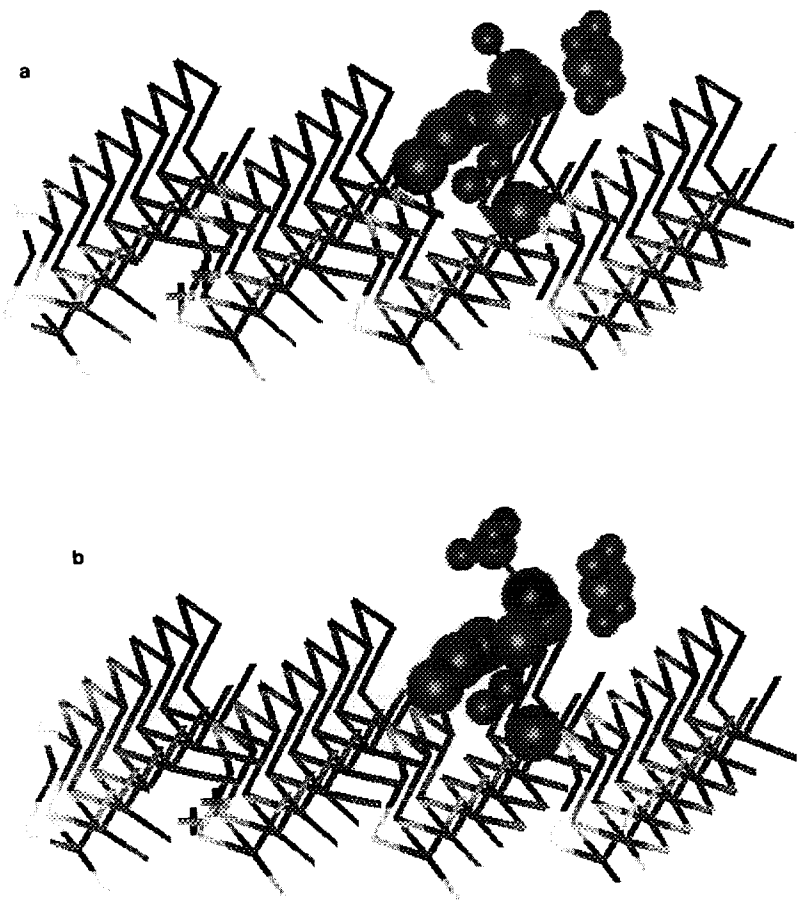

FIG. 6. The calculated structures of the C_2H_4 monomer interacting with adsorbed (a) $TiCl_2H$ and (b) $TiCl_2CH_3$ species on the (100) surface of the β-$MgCl_2$ crystal.

TABLE 6

Calculated Structural Parameters and Binding Energies of C_2H_4 Monomer Interacting in Two Ways (*para* and *ortho*) with Adsorbed $TiCl_2CH_3$ Molecule on the (110) Surface of β-$MgCl_2$

Species	Method/basis sets	R_{Ti-C} (Å)[a]	$R_{C=C}$ (Å)[b]	E_{bind} (eV)[c]
$C_2H_4/TiCl_2CH_3$	RHFOS/MIN	3.494	1.448	0.348
(*para*)	RHFOS/DZ	3.497	1.362	0.283
$C_2H_4/TiCl_2CH_3$	RHFOS/MIN	3.610	1.449	0.220
(*ortho*)	RHFOS/DZ	3.510	1.358	0.177

[a] The distance between the middle point of the C=C double bond and the Ti atom in the $TiCl_2CH_3$.

[b] The bond length of the C=C double bond.

[c] E_{bind} is calculated by subtracting the total energy of the Ti–C_2H_4 species adsorbed on the surface from the total energies of both the Ti species adsorbed on the surface and the isolated C_2H_4 molecule.

lier, due to the atomic arrangement of both the (100) and the (110) surfaces of the β-$MgCl_2$ crystal, $TiCl_2R$ (R = H, CH_3, and Cl) will interact with these surfaces by forming (1) double-Cl bridges to saturate the coordination sites around the Mg atoms and (2) the weaker Ti–Cl bond to saturate the coordination site around the Ti centre. As a result the activity of unsaturated coordination sites of Ti species for interaction with C_2H_4 will depend on the atomic arrangement of the surface structures; that is, different surface structures could promote different activities for Ti interaction with the C_2H_4 monomer.

We will first consider the interaction between C_2H_4 and $TiCl_2R$ species adsorbed on the (100) surface. Our calculated binding energies, as shown in Table 5, suggest that the interaction between these Ti species and the C_2H_4 monomer is energetically favourable. We attribute the strong interaction to the electron transfer from the Ti centre to the π^* antibonding orbital of C_2H_4, as can be seen from the increase of the bond length of C=C shown in Table 5. The formation of the weak Ti–Cl bond manifested by the slightly distorted trigonal planar $TiCl_2R$, as shown in Fig. 6, will facilitate this interaction as noted above.

The influence of surface structure on the coordination of ethylene to Ti complexes is clearly shown by calculating both geometries and binding energies of C_2H_4 interacting with the $TiCl_2CH_3$ species adsorbed on the (110) surface. From our calculated binding energies shown in Table 6 we find that the binding energy for the C_2H_4 monomer to the Ti centre decreases significantly on the (110) relative to the (100) surface. The likely explanation for this effect is that the structure of the $TiCl_2CH_3$ species remains undistorted trigonal planar when adsorbed on the (110) surface. As a result the C_2H_4 monomer will not interact with Ti species adsorbed on this surface as effectively, due to the steric effect of the interactions with the (110) surface and the CH_3 group in the $TiCl_2CH_3$ molecule. Our calculated longer bond lengths for Ti–C and shorter bond lengths for C=C, as shown in Table 6, support this argument.

Finally, we investigated the different conformations of the C_2H_4 monomer with respect to the $TiCl_2CH_3$ species adsorbed on the (110) surface to help us understand the initial stage of the insertion of the C_2H_4 molecule into the Ti–CH_3 σ bond. The C_2H_4 molecule has to rotate from the configuration (*para*) shown in Fig. 7a to the configuration (*ortho*) shown in Fig. 7b to allow the insertion reaction to take place. We therefore compare the energy difference between these two configurations as reported in Table 6. The very small energy difference (which is less than 0.15 eV) suggests that the C_2H_4 molecule can rotate very easily to either configuration at moderate temperatures.

CONCLUSIONS

Point-charge embedded quantum mechanical cluster techniques have been successfully applied to the Ti/$MgCl_2$-

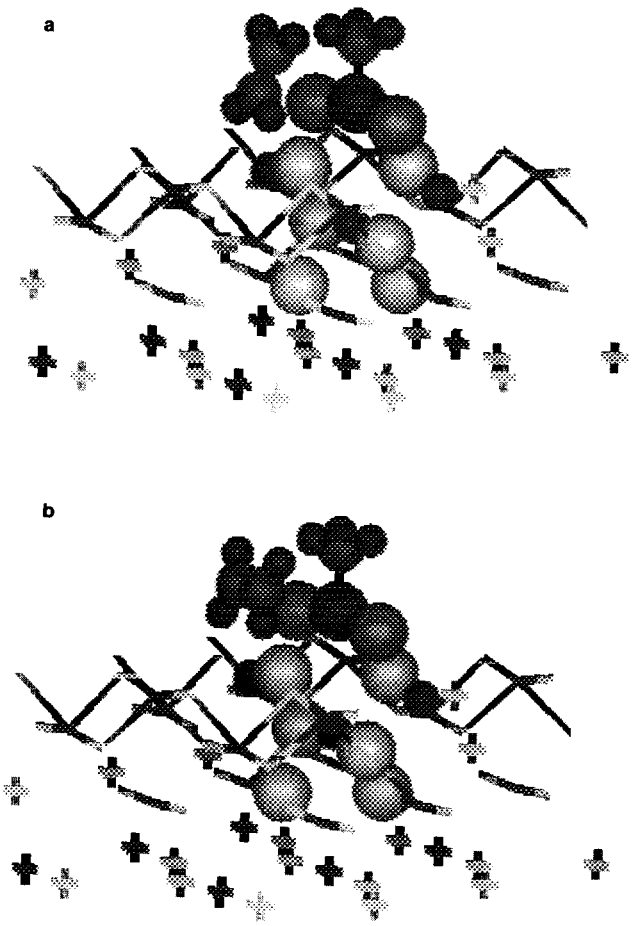

FIG. 7. The calculated structures of (a) C_2H_4 (*para*) and (b) C_2H_4 (*ortho*) monomer interacting with the adsorbed $TiCl_2CH_3$ species on the (110) surface of the β-$MgCl_2$ crystal.

supported Ziegler–Natta catalysts. We first modelled quantum mechanically both the (100) and (110) surfaces of the β-$MgCl_2$ crystal using both Mg_2Cl_4 and Mg_3Cl_6 clusters with a finite size of point charges. We have analysed how different oxidation states of Ti (III and IV) will affect the geometries and energetics of Ti complexes adsorbed on the surfaces of the β-$MgCl_2$ crystal. Our calculated results clearly indicate that the Ti(III) complexes will be adsorbed more strongly than those of Ti(IV) on the surface of the (100) plane. To demonstrate the effect of the surface structure on the stability of Ti species adsorbed on the surface of the β-$MgCl_2$ crystal we studied the geometries and energetics of $TiCl_2R$ species adsorbed on both (100) and (110) surfaces of β-$MgCl_2$ crystal. Our calculated results found that the structure of the (110) surface enhances the interaction between the Ti atom within the $TiCl_2R$ and the Cl atoms on the (110) surface to promote even stronger absorbtion of $TiCl_2R$ species on that surface. Finally, our calculated geometries and energies of precoordinated-ethylene Ti(III) complexes adsorbed on the different surfaces suggest that the less stable Ti complexes adsorbed on the (100) surface will promote the formation of more stable precoordinated-ethylene Ti complexes on that surface.

ACKNOWLEDGMENTS

We are grateful to B.P. (British Petroleum) for financial support and to Drs. P. Maddox, A. Foakes, and J. McNally for useful discussions. We would also like to thank Dr. P. Sherwood for modifying the GAMESS program to allow us to use the pseudopotential for point-charge embedded cluster calculations. Finally we wish to thank Dr. S. Hill and Mr. D. Lewis for their assistane in setting up the point-charge arrays used in this study.

REFERENCES

1. For reviews and discussions of the $Ti/MgCl_2$ catalytic system see Barbe, P. C., Cecchin, G., and L. Noristi, *Adv. Polym. Sci.* **81,** 1 (1987).
2. Sivaram, S., *Ind. Eng. Chem. Prod. Res. Dev.* **2,** 121 (1977).
3. Chien, J. C. W., and Hsieh, J. T. T., *J. Polym. Sci. Polym. Chem. Ed.* **14,** 1915 (1976).
4. Giannini, U., *Makromol. Chem. Suppl.* **5,** 216 (1981).
5. Galli, P. Barbe, P. C., Guidetti, G. P., Zannetti, R., Martorana, A., Marigo, A., Bergozza, M., and Fischera, A., *Eur. Polym. J.* **19,** 19 (1984).
6. Kashiwa, N., and Yoshitake, J., *Makromol. Chem.* **185,** 1133 (1984).
7. Chien, J. C. W., and Wu, J. C., *J. Polym. Sci. Polym. Chem. Ed.* **20,** 2461 (1982).
8. Chien, J. C. W., Wu, J. C., and Kuo, C. I., *Polym. Sci. Polym. Chem. Ed.* **20,** 2019 (1982).
9. Weber, S., Chien, J. C. W., and Hu, Y., *in* "Transition Metals and Organometallics as Catalysts for Olefin Polymerization" (W. Kaminsky and H. Sinn, Eds.). Springer-Verlag, Berlin/Heidelberg, 1988.
10. Gerbasi, R., Marigo, A., Martorana, A., Zannetti, R., Guidetti, G. P., and Baruzzi, *Eur. Polym. J.* **20,** 967 (1984).
11. Lin, J. S., and Catlow, C. R. A., *J. Mater. Chem.* **3,** 1217 (1993).
12. Colbourn, E. A., Cox, P. A., Carruthers, B., and Jones, P. J. V., *J. Mater. Chem.* **4,** 805 (1994).
13. Colbourn, E. A., *Adv. Solid State Chem.* **1,** 1 (1989).
14. GAMESS-UK is a package of *ab initio* programs written by Guest, M. F., van Lenthe, J. H., Kendrick, J., Schoffel, K., Sherwood, P., and Harrison, R. J., with contributions from Amos, R. D., Buenker, R. J., Dupuis, M., Handy, N. C., Hillier, I. H., Knowles, P. J., Bonacic-Koutecky, V., Niessen, W. von, Saunders, V. R., and Stone, A. J. The package is derived from the original GAMESS code, Dupuis, M., Spangler, D., and Wendoloski, J., "NRCC Software Catalog," Vol. 1, Program QG01 (GAMESS), 1980.
15. Hay, P. J., and Wadt, W. R., *J. Chem. Phys.* **82,** 270, 284, 299 (1985).